

## Observation of ${}^4_{\Lambda}\text{H}$ Hyperhydrogen by Decay-Pion Spectroscopy in Electron Scattering

A. Esser,<sup>1</sup> S. Nagao,<sup>2</sup> F. Schulz,<sup>1</sup> P. Achenbach,<sup>1,†</sup> C. Ayerbe Gayoso,<sup>1</sup> R. Böhm,<sup>1</sup> O. Borodina,<sup>1,3</sup> D. Bosnar,<sup>4</sup> V. Bozkurt,<sup>3</sup> L. Debenjak,<sup>5</sup> M. O. Distler,<sup>1</sup> I. Friščić,<sup>4</sup> Y. Fujii,<sup>2</sup> T. Gogami,<sup>2,‡</sup> O. Hashimoto,<sup>2,\*</sup> S. Hirose,<sup>2</sup> H. Kanda,<sup>2</sup> M. Kaneta,<sup>2</sup> E. Kim,<sup>3</sup> Y. Kohl,<sup>1</sup> J. Kusaka,<sup>2</sup> A. Margaryan,<sup>6</sup> H. Merkel,<sup>1</sup> M. Mihovilović,<sup>1</sup> U. Müller,<sup>1</sup> S. N. Nakamura,<sup>2</sup> J. Pochodzalla,<sup>1</sup> C. Rappold,<sup>3,7</sup> J. Reinhold,<sup>8</sup> T. R. Saito,<sup>1,3,7</sup> A. Sanchez Lorente,<sup>7</sup> S. Sánchez Majos,<sup>1</sup> B. S. Schlimme,<sup>1</sup> M. Schoth,<sup>1</sup> C. Sfienti,<sup>1</sup> S. Širca,<sup>5</sup> L. Tang,<sup>9</sup> M. Thiel,<sup>1</sup> K. Tsukada,<sup>2,§</sup> A. Weber,<sup>1</sup> and K. Yoshida<sup>3</sup>

(A1 Collaboration)

<sup>1</sup>*Institut für Kernphysik, Johannes Gutenberg-Universität, D-55099 Mainz, Germany*

<sup>2</sup>*Department of Physics, Tohoku University, Sendai, 980-8571, Japan*

<sup>3</sup>*GSI Helmholtz Centre for Heavy Ion Research, D-64291 Darmstadt, Germany*

<sup>4</sup>*Department of Physics, University of Zagreb, HR-10002 Zagreb, Croatia*

<sup>5</sup>*Department of Physics, University of Ljubljana, and Jožef Stefan Institute, SI-1000 Ljubljana, Slovenia*

<sup>6</sup>*Yerevan Physics Institute, 375036 Yerevan, Armenia*

<sup>7</sup>*Helmholtz Institute Mainz, D-55099 Mainz, Germany*

<sup>8</sup>*Department of Physics, Florida International University, Miami, Florida 33199, USA*

<sup>9</sup>*Department of Physics, Hampton University, Hampton, Virginia 23668, USA*

(Received 27 January 2015; published 9 June 2015)

At the Mainz Microtron MAMI, the first high-resolution pion spectroscopy from decays of strange systems was performed by electron scattering off a  ${}^9\text{Be}$  target in order to study the  $\Lambda$  binding energy of light hypernuclei. Positively charged kaons were detected by a short-orbit spectrometer with a broad momentum acceptance at  $0^\circ$  forward angles with respect to the beam, efficiently tagging the production of strangeness in the target nucleus. Coincidentally, negatively charged decay pions were detected by two independent high-resolution spectrometers. About  $10^3$  pionic weak decays of hyperfragments and hyperons were observed. The pion momentum distribution shows a monochromatic peak at  $p_\pi \approx 133 \text{ MeV}/c$ , corresponding to the unique signature for the two-body decay of hyperhydrogen  ${}^4_{\Lambda}\text{H} \rightarrow {}^4\text{He} + \pi^-$ , stopped inside the target. Its  $\Lambda$  binding energy was determined to be  $B_\Lambda = 2.12 \pm 0.01 \text{ (stat)} \pm 0.09 \text{ (syst)} \text{ MeV}$  with respect to the  ${}^3\text{H} + \Lambda$  mass.

DOI: 10.1103/PhysRevLett.114.232501

PACS numbers: 21.80.+a, 13.75.Ev, 21.10.Dr, 29.30.Ep

**Introduction.**—When a  $\Lambda$  hyperon replaces one of the nucleons ( $N = n$  or  $p$ ) in the nucleus, a bound system can be formed by the hyperon and the core of the remaining nucleons,  $\Lambda$  hypernucleus. The  ${}^4_{\Lambda}\text{H}$  nucleus is a heavy isotope of the element hydrogen, in which a  $\Lambda$  hyperon is bound to a tritium core. It was found in early helium bubble chamber [1] and nuclear emulsion experiments [2–5]. In a ground state, a hypernucleus decays to a nonstrange nucleus through mesonic (MWD) or nonmesonic weak decay modes. By detecting the decay of hypernuclei and measuring the momenta of the decay products, the binding energies of the  $\Lambda$  hyperon, i.e., the  $\Lambda$  separation energy, for a larger number of  $s$ - and  $p$ -shell hypernuclei were reported in the 1960s and 1970s.

Precise determination of the binding energies of hypernuclei can be used to test the  $YN$  interactions ( $Y = \Lambda$  or  $\Sigma$ ) in many-body systems. Contrary to the nonstrange sector, where a large database is used to successfully model the  $NN$  forces, the available data on  $YN$  scattering is not sufficient to determine realistic interactions among

hyperons and nucleons. Various hypernuclear structure theories exist in which the binding energies of light hypernuclei are calculated; most recent approaches include cluster models and *ab initio* calculations with the interactions constructed either in the meson-exchange picture or within chiral effective field theory [6–11]. Measuring the binding energy splitting in the mass  $A = 4$  hypernuclei,  ${}^4_{\Lambda}\text{H}$  and  ${}^4_{\Lambda}\text{He}$ , is especially helpful for investigating the origin of charge symmetry breaking in the strong interaction [12,13].

The most abundant decay of  ${}^4_{\Lambda}\text{H}$  observed in nuclear emulsions is the charged two-body mode  ${}^4_{\Lambda}\text{H} \rightarrow {}^4\text{He} + \pi^-$ . However, it could not be used to deduce the binding energy because of the larger systematic error in the pion range–energy relation for pion ranges greater than 3 cm [4]. Instead, only  $\sim 160$  three-body decays were used. References [2–4] evaluated 21, 63, and 56 events from  ${}^4_{\Lambda}\text{H} \rightarrow \pi^- + {}^1\text{H} + {}^3\text{H}$  and only 2, 7, and 11 events from  ${}^4_{\Lambda}\text{H} \rightarrow \pi^- + {}^2\text{H} + {}^2\text{H}$ , respectively. In Ref. [4] the binding energies of decays from these two decay modes were

reported separately to be  $1.92 \pm 0.12$  and  $2.14 \pm 0.07$  MeV with a difference of  $0.22 \pm 0.14$  MeV. The FWHM of the distribution of  ${}^4_\Lambda\text{H}$  binding energies is 2.1 MeV. Despite extensive calibrations, systematic uncertainties of at least 0.05 MeV in the binding energies should be assumed for emulsion data [14]. In Ref. [2] a possible systematic error of 0.15 MeV is quoted. From these ambiguities it is evident that independent, high-resolution experiments are needed to confirm the emulsion data on binding energies.

This Letter presents the first result of the measurement of a  $\Lambda$  binding energy in light hypernuclei from pionic decays in electron scattering. Pions were detected in high-resolution spectrometers measuring the momentum with much better resolution than with emulsion and with completely independent systematical uncertainties.

*Measurement technique.*—In reaction spectroscopy, ground and excited hypernuclear states can be identified by a missing mass analysis of the incident beam and the associated reaction meson. Since these reactions require stable target nuclei, hypernuclei accessible by these reactions are limited. The direct reaction spectroscopy of  ${}^4_\Lambda\text{H}$  is not possible using charged meson beams in the established ( $\pi^+$ ,  $K^+$ ) and ( $K^-$ ,  $\pi^-$ ) reactions. The first observation of  ${}^4_\Lambda\text{H}$  bound states in missing mass spectroscopy using the ( $e$ ,  $e'K^+$ ) reaction was reported a decade ago [15]. This pioneering experiment reached a mass resolution of 4 MeV/ $c^2$ . Only few precision measurements of  $\Lambda$  binding energies were conducted at Jefferson Lab, most recently the spectroscopy of  ${}^7_\Lambda\text{He}$  that achieved a binding energy resolution of  $\sim 0.6$  MeV [16].

The first counter experiments detecting the two-body MWD of  ${}^4_\Lambda\text{H}$  were performed at KEK in the 1980s and 1990s [17,18]. From the observed decay-pion peak at  $132.6 \pm 0.3$  MeV/ $c$ , a binding energy of  $2.35 \pm 0.22$  MeV can be calculated. In this experiment, strangeness was exchanged with nuclei by  $K^-$  absorption within a thick target so that the momentum resolution of 1.9–3.3 MeV/ $c$  FWHM was not competitive to the emulsion data in determining the  $\Lambda$  binding energy.

In 2007, the usage of magnetic spectrometers to measure the momenta of pions from two-body decays of light hypernuclei fragmented from the excited states of initially electroproduced hypernuclei was proposed for Jefferson Lab [19]. An electroproduced hypernucleus can have excitation energies above the lowest particle emission threshold and then lose excitation energy through fragmentation, i.e., nucleon or cluster emission. This is a very fast process that can lead to particle-stable hypernuclei in a large range of mass and atomic numbers, including hyperisotopes which are not accessible in missing-mass experiments. MWD takes place from the ground state of these hypernuclei. The pion momenta from two-body MWD of the lightest systems ( $A \leq 9$ ) are  $p_\pi \sim 96$ –138 MeV/ $c$ . The mass of a hypernucleus can be obtained from a

measurement of  $p_\pi$ . Kaons can be tagged to suppress nonstrange processes.

*Experiment.*—The experiment was carried out by the A1 Collaboration at the spectrometer facility (see Refs. [20,21] for a detailed description of the spectrometers) at the Mainz Microtron MAMI-C, in Germany, with a 1.508 GeV electron beam incident on a 125  $\mu\text{m}$  thick and  $54^\circ$  tilted  ${}^9\text{Be}$  target foil with a beam current of 20  $\mu\text{A}$ . The layout of the experimental setup is shown in Fig. 1, and details can be found in Ref. [22]. The luminosity corrected for the data acquisition dead time was  $\int \mathcal{L} dt \sim 235 \text{ fb}^{-1}$ , integrated over a period of  $\sim 250$  h during the year 2012. The total charge of the electrons hitting the target was 18.2 C.

Pions were detected with two high-resolution spectrometers (SpekA and SpekC) with quadrupole-sextupole-dipole-dipole configuration and a  $\Omega_\pi^{\text{lab}} = 28$  msr solid angle acceptance each, in which vertical drift chambers were used for tracking, scintillation detectors for triggering and timing, and gas Cerenkov detectors for discrimination between electrons and pions. The vertical drift chambers are capable of measuring a particle track with effective position and angle resolutions of  $\sigma_x = 180 \mu\text{m}$  and  $\sigma_\theta = 1.0$  mrad. The spectrometers achieve a relative momentum resolution of  $\delta p/p \sim 10^{-4}$  and were operated at central momenta of 115 and 125 MeV/ $c$  with momentum acceptances of  $\Delta p/p = 20\%$  (SpekA) and 25% (SpekC). The survival probabilities of pions at these momenta are  $\epsilon_\pi \sim 0.3$ .

The tagging of kaons was performed by the Kaos spectrometer. It was positioned at  $0^\circ$  with respect to the electron beam direction. The central momentum was 924 MeV/ $c$ , covering a momentum range of  $\Delta p/p = 50\%$  with a solid angle acceptance of  $\Omega_K^{\text{lab}} = 16$  msr. The

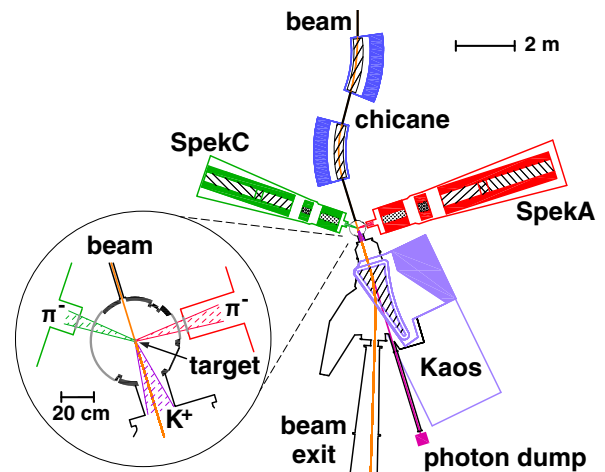


FIG. 1 (color online). Layout of the setup showing the electron beam line, the two high-resolution spectrometers SpekA and SpekC used for pion detection in the backward hemisphere, and the Kaos spectrometer at  $0^\circ$  angle relative to the outgoing beam used for kaon tagging. The beam enters from the top. The inset shows an enlarged view of the scattering chamber and the detected particles names.

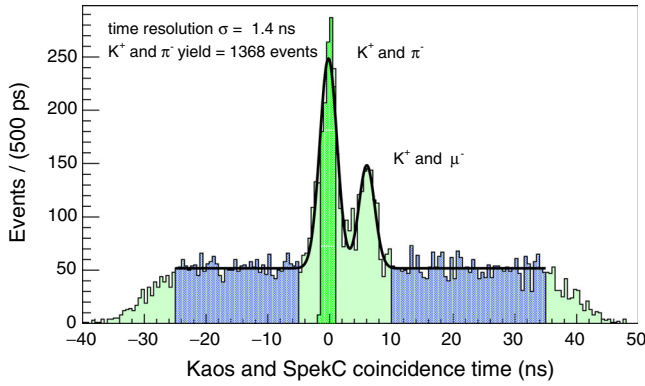


FIG. 2 (color online). Coincidence time spectrum for  $K^+$  in the Kaos spectrometer and  $\pi^-$  or  $\mu^-$  in SpekC, after correcting for the reconstructed flight path lengths of  $K^+$  and  $\pi^-$  through the spectrometers. The time gates for selecting true (2.5 ns width) and accidental coincidences (45 ns width) are indicated by different colors. The solid line represents a fit to the spectrum with two Gaussian shaped peaks each on top of an accidental background distribution. The peaks were resolved with  $\sigma_t \sim 1.4$  ns resolution.

detector system includes segmented scintillator walls for tracking, energy-loss determination, and timing. Two aerogel Čerenkov detectors were used for pion rejection with a combined 94% efficiency when keeping the kaon rejection lower than 1%. The kaon survival probability was  $\epsilon_K \approx 0.40$  for a flight path of 6.45 m. The time of flight was measured inside the spectrometer with a resolution of  $\sigma_t \approx 180$  ps along flight paths of 1–1.5 m. The experimental challenge in this experiment was originated by the positrons from pair production with large cross sections near  $0^\circ$ . The resulting high flux of background positrons in the spectrometer was reduced by several orders of magnitude by using a lead absorber with its thickness up to  $t = 25X_0$  radiation lengths [22]. The detection loss for the kaons in this absorber amounted to  $\eta_{\text{lead}} \sim 70\%$ .

**Data analysis.**—The pion momentum, its direction, and the reaction vertex were reconstructed from the focal plane coordinates using the well-known backward transfer matrices describing the spectrometer optics. The momenta of the outgoing pions were corrected for energy loss inside the target, a few cm thick of air, and two vacuum window foils 120  $\mu\text{m}$  thick each. Kaons were identified by their specific energy loss  $dE/dx$  and velocity  $\beta$  from the time of flight.

Figure 2 shows the coincidence time between  $K^+$  in the Kaos spectrometer and  $\pi^-$  or  $\mu^-$  in SpekC. The prominent peak at zero time includes  $10^3$  pions while the peak of muons is originated by the decay events of pions. True coincidence events were selected from a time gate with a width of 2.5 ns. Accidental coincidence events from the two coincidence time sidebands of 45 ns total width were used to evaluate the accidental background height and shape in the momentum distribution.

The top panel of Fig. 3 shows the distribution of available data on the  $\Lambda$  hyperon binding energy in  ${}^4_\Lambda\text{H}$

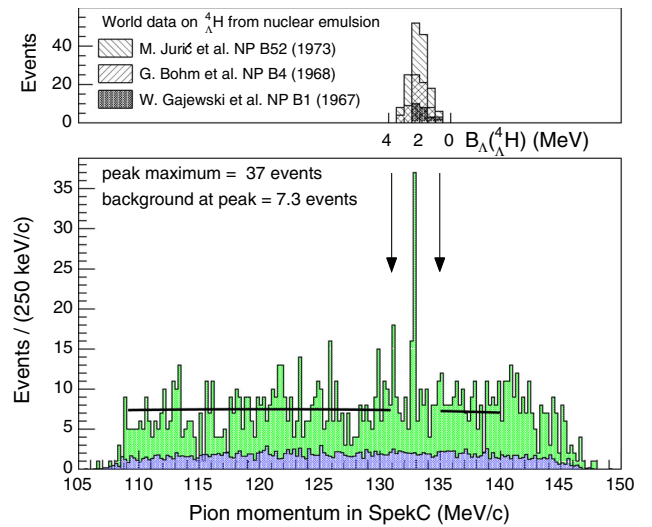


FIG. 3 (color online). Pion momentum distribution in SpekC for true coincidences (green) and accidental coincidences (blue) scaled by the ratio of the time gate widths. A monochromatic peak at  $p_\pi \approx 133$  MeV/c was observed, which is a unique signature for the two-body decay of stopped  ${}^4_\Lambda\text{H} \rightarrow {}^4\text{He} + \pi^-$ . The top panel shows on the corresponding binding energy scale the distribution of data on the  $\Lambda$  hyperon binding energy in  ${}^4_\Lambda\text{H}$  from emulsion experiments [2–4]. Arrows indicate the region of interest in the momentum spectrum.

from emulsion experiments [2–4], where the compilation in Ref. [4] includes reanalyzed events from Refs. [2,3]. The width of this distribution from  $B_\Lambda > 0.5$  MeV to  $B_\Lambda < 3.5$  MeV defines a region of interest corresponding to the momenta of two-body decay pions for stopped  ${}^4_\Lambda\text{H}$ :  $131 < p_\pi < 135$  MeV/c.

The bottom panel of Fig. 3 shows the pion momentum distribution in SpekC for the events within the true coincidence time gate. The measured pion momentum distribution in the time sidebands was scaled by the ratio of the time gate widths, giving  $1.8 \pm 0.1$  accidental events/bin. The exceeding background was produced by MWD of strange systems, the only reaction that can generate coincident events meeting the kinematical conditions. The distribution outside of the region of interest was fitted with a single scale factor to a template function  $b$  which was determined by a Monte Carlo simulation of MWD events including angular and energy dependencies of kaon production in electron scattering off  ${}^9\text{Be}$ . In the simulation, the elementary cross sections for  $p(\gamma, K^+)\Lambda$ ,  $p(\gamma, K^+)\Sigma^0$ , and  $n(\gamma, K^+)\Sigma^-$  were taken from the K-Maid model [23,24], which describes available kaon photoproduction data. The Fermi-motion effects that modify the elementary cross sections for the Be target were calculated in the incoherent impulse approximation. In the simulated spectrum  $\Lambda$  decay pions are dominating in the range 20–110 MeV/c,  $\Sigma^-$  decay pions are dominating in the range 110–194 MeV/c, and at 194.3 MeV/c the monochromatic peak of stopped  $\Sigma^-$  decays is found. Inside the

momentum and angular acceptances of the spectrometer the background spectrum is featureless and its momentum dependence is practically flat. From the fit result 5.5 events/bin can be attributed to  $\Sigma^-$  decays in the measured spectrum.

A localized excess of events over this background was observed inside the region of interest near to  $p_\pi \approx 133$  MeV/c that is a unique signature for  ${}^4_\Lambda\text{H} \rightarrow {}^4\text{He} + \pi^-$ . The region of interest for  ${}^4_\Lambda\text{H}$  was not inside the acceptance of SpekA.

*Result and discussion.*—Figure 4 shows the pion momentum distribution in SpekC in the region of interest. The spectrum was fitted by a function that is composed of a signal  $s$  that is formed by a Landau distribution representing the known energy loss convoluted with a Gaussian resolution function on top of the known background  $b$ , minimizing the negative logarithm of the likelihood  $L(s+b)$ . The spectrum was also fitted with the background-only function. The corresponding significance level of the signal calculated via the likelihood ratio following Ref. [25] is  $S_L = \sqrt{-2 \ln[L(b)/L(s+b)]} = 5.2$ . The shape of the peak was derived from the simulations of the energy loss of pions along their tracks with a most probable energy loss of  $\Delta E \sim 0.140 \pm 0.005$  MeV. The width of the peak was observed to be FWHM  $\sim 0.15$  MeV/c, which is consistent with the prediction. The largest contribution to the width was from multiple scattering of the pions inside the target and at the two vacuum window foils. Uncertainties in the backward transfer matrix contribute less.

Systematic differences due to the fitting procedure were estimated by using different probability distribution functions to describe the peak shape, different fit methods (unbinned and binned) and minimizers, different fit regions, and different parametrizations of the background. The most probable momentum for the decay-pion peak was within  $\delta p < 10$  keV/c for all cases.

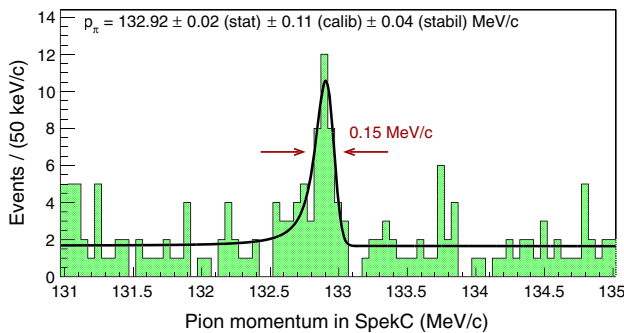


FIG. 4 (color online). Pion momentum distribution in SpekC in the region of interest with a fit composed of a Gaussian resolution function convoluted with a Landau distribution representing the energy loss on top of the background function. The observed signal shape and width are consistent with the simulation.

The peak position,  $p_\pi = 132.92$  MeV/c, of the signal was converted to  $\Lambda$  hyperon binding energy  $B_\Lambda$  using

$$M({}^4_\Lambda\text{H}) = \sqrt{M^2({}^4\text{He}) + p_\pi^2} + \sqrt{M_\pi^2 + p_\pi^2} \quad \text{and} \\ B_\Lambda = M({}^3\text{H}) + M_\Lambda - M({}^4_\Lambda\text{H}), \quad \text{with } c = 1,$$

where the known nuclear masses,  $M({}^3\text{H}) = 2808.921$  MeV and  $M({}^4\text{He}) = 3727.379$  MeV, were obtained from tabulated mass excess values [26] and the charged pion mass  $M_\pi = 139.570$  MeV and  $\Lambda$  hyperon mass  $M_\Lambda = 1115.683$  MeV from the latest Particle Data Group publication [27].

The calibration of the momentum spectra has been performed with a 195.17 MeV electron beam using the  ${}^{181}\text{Ta}(e, e')$  elastic scattering as well as the inelastic spectrum of the  ${}^{12}\text{C}(e, e')$  reaction to check the linearity of the momentum scale. The momentum was referenced against the beam energy. The beam energy was measured with an absolute accuracy of  $\delta E_{\text{beam}} = \pm 0.16$  MeV by exact determination of the beam position on the accelerator axis and in a higher return path. The uncertainty on the beam energy translates into a calibration uncertainty of  $\delta p_{\text{calib}} = \pm 0.11$  MeV/c. This is the dominant source of systematic uncertainty in the binding energy. Uncertainties in the spectrometer angle were insignificant. The backward transfer matrices were checked using sieve slit data. The stability of the magnetic field in the spectrometers, checked with regular Hall probe and NMR probe measurements, showed relative variations of the order  $10^{-4}$  that translate into a systematic uncertainty,  $\delta p_{\text{stabil}} = \pm 0.04$  MeV/c, in the momentum. A total systematic uncertainty of 0.09 MeV for the binding energy was obtained using the kinematical relation  $dB_\Lambda/c \approx -0.725 dp_\pi$  for  ${}^4_\Lambda\text{H}$ . The final result is then  $B_\Lambda = 2.12 \pm 0.01$  (stat)  $\pm 0.09$  (syst) MeV with respect to the  ${}^3\text{H} + \Lambda$  mass.

In the present experiment, the momentum acceptance of the pion spectrometers covered the monochromatic decay momenta of  ${}^{3,4,6}_\Lambda\text{H}$ ,  ${}^{6,7}_\Lambda\text{He}$ , and  ${}^{7-9}_\Lambda\text{Li}$ , including very neutron-rich nuclei. A statistical decay model was applied to evaluate the relative yields [22]. From the range of kinetic energies of the different hypernuclei, the stopping probabilities inside the target were determined:  $P_{\text{stop}} \sim 40\%$  for hyperhydrogen isotopes, 70%–80% for hyperhelium isotopes, and  $\sim 90\%$  for hyperlithium isotopes.  ${}^4_\Lambda\text{H}$  has a large total  $\pi^-$  decay width, comparable to the free  $\Lambda$  decay width,  $\Gamma_{\pi^-}/\Gamma_\Lambda = 1.00^{+0.18}_{-0.15}$ , and the relative partial decay width of the two-body mode,  $\Gamma_{\pi^-+{}^4\text{He}}/\Gamma_{\pi^-} = 0.69 \pm 0.02$  [18]. These widths are larger than for all other known light hyperisotopes.

Detection of the pionic decay of  ${}^4_\Lambda\text{H}$  has been achieved for the first time in electroproduction and for the first time using a spectrometer with  $10^{-4}$  relative momentum resolution. This resolution is about a factor 10 better than for the emulsion data. Figure 5 shows a compilation of the  $\Lambda$

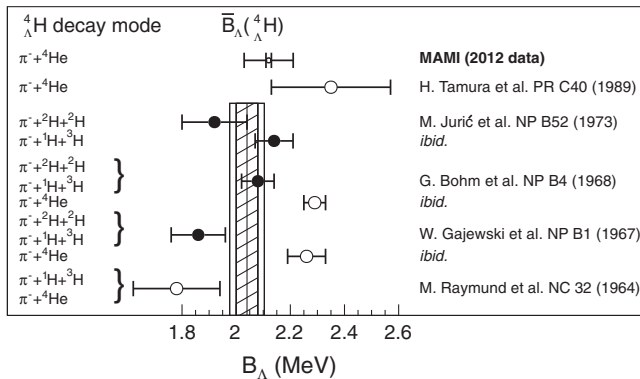


FIG. 5. Measured  $\Lambda$  binding energies of  ${}^4_\Lambda\text{H}$  evaluated from pionic decays [2–4,17,28]. Full circles present values from three-body decays, open circles from two-body decays, errors on the emulsion data are statistical only. The binding energy value from Ref. [17] was calculated from the observed momentum of  $132.6 \pm 0.3$  MeV/c. The mean value as compiled by Ref. [4] excludes data from the two-body decay mode and is shown by the vertical bands with statistical and total errors. The uncertainties on the MAMI value are statistical (inner) and total (outer).

binding energy of  ${}^4_\Lambda\text{H}$  evaluated from pionic decays. It was demonstrated that the use of high-resolution spectrometers at a high intensity beam provides a novel and independent technique to determine the  $\Lambda$  binding energies of light hypernuclei.

This work was supported in part by Deutsche Forschungsgemeinschaft (SFB 1044), the Carl Zeiss Foundation, European Community Research Infrastructure Integrating Activity FP7, U.S.-DOE Contract No. DEFG02-97ER41047, the Strategic Young Researchers Overseas Visits Program for Accelerating Brain Circulation (R2201), and the Core-to-Core program (21002) of JSPS.

\*Deceased.

†patrick@kph.uni-mainz.de

‡Present address: Graduate School of Science, Kyoto University, Kyoto 606-8502, Japan.

§Present address: Research Center for Electron Photon Science, Tohoku University, Sendai 982-0826, Japan.

- [1] M. M. Block *et al.*, in *Proceedings of the International Conference on Hyperfragments, St. Cergue, Switzerland, 1963* (CERN, Geneva, 1964), pp. 63–74.
- [2] W. Gajewski *et al.*, *Nucl. Phys.* **B1**, 105 (1967).
- [3] G. Bohm *et al.*, *Nucl. Phys.* **B4**, 511 (1968).
- [4] M. Jurić *et al.*, *Nucl. Phys.* **B52**, 1 (1973).
- [5] D. Bertrand, G. Coremans, C. Mayeur, J. Sacton, P. Vilain, G. Wilquet, J. H. Wickens, D. O'Sullivan, D. H. Davis, and J. E. Allen, *Nucl. Phys.* **B16**, 77 (1970).
- [6] E. Hiyama, M. Kamimura, T. Motoba, T. Yamada, and Y. Yamamoto, *Phys. Rev. C* **65**, 011301(R) (2001).
- [7] A. Nogga, H. Kamada, and W. Glöckle, *Phys. Rev. Lett.* **88**, 172501 (2002).
- [8] H. Nemura, Y. Akaishi, and Y. Suzuki, *Phys. Rev. Lett.* **89**, 142504 (2002).
- [9] E. Hiyama, Y. Yamamoto, T. Motoba, and M. Kamimura, *Phys. Rev. C* **80**, 054321 (2009).
- [10] R. Wirth, D. Gazda, P. Navrátil, A. Calci, J. Langhammer, and R. Roth, *Phys. Rev. Lett.* **113**, 192502 (2014).
- [11] J. Haidenbauer, U.-G. Meißner, A. Nogga, and H. Polinder, *Lect. Notes Phys.* **724**, 113 (2007).
- [12] A. Nogga, *Nucl. Phys.* **A914**, 140 (2013).
- [13] A. Gal, *Phys. Lett. B* **744**, 352 (2015).
- [14] D. H. Davis, *Nucl. Phys.* **A547**, 369 (1992).
- [15] F. Dohrmann *et al.* (E91-016 Collaboration), *Phys. Rev. Lett.* **93**, 242501 (2004).
- [16] S. N. Nakamura *et al.* (HKS (JLab E01-011) Collaboration), *Phys. Rev. Lett.* **110**, 012502 (2013).
- [17] H. Tamura *et al.*, *Phys. Rev. C* **40**, R479 (1989).
- [18] H. Outa, M. Aoki, R. S. Hayano, T. Ishikawa, M. Iwasaki, A. Sakaguchi, E. Takada, H. Tamura, and T. Yamazaki, *Nucl. Phys.* **A639**, 251c (1998).
- [19] L. Tang *et al.*, Proposal No. E08-012, Jefferson Lab, 2007.
- [20] P. Achenbach (A1 Collaboration), *Eur. Phys. J. Spec. Top.* **198**, 307 (2011).
- [21] K. I. Blomqvist *et al.* (A1 Collaboration), *Nucl. Instrum. Methods Phys. Res., Sect. A* **403**, 263 (1998).
- [22] A. Esser *et al.* (A1 Collaboration), *Nucl. Phys.* **A914**, 519 (2013).
- [23] T. Mart and C. Bennhold, *Phys. Rev. C* **61**, 012201(R) (1999).
- [24] T. Mart, *Phys. Rev. C* **62**, 038201 (2000).
- [25] R. D. Cousins, J. T. Linnemann, and J. Tucker, *Nucl. Instrum. Methods Phys. Res., Sect. A* **595**, 480 (2008).
- [26] G. Audi, A. H. Wapstra, and C. Thibault, *Nucl. Phys.* **A729**, 337 (2003).
- [27] K. A. Olive *et al.* (Particle Data Group), *Chin. Phys. C* **38**, 090001 (2014).
- [28] M. Raymund, *Nuovo Cimento* **32**, 555 (1964).